Available online at www.sciencedirect.com
SCIENCE DIRECT®
ELSEVIER
Journal of Magnetism and Magnetic Materials 286 (2005) 216–219
Journal of magnetism and magnetic materials
www.elsevier.com/locate/jmmm

Enhanced exchange bias in ferromagnet/antiferromagnet multilayers

Amitesh Paul* , Daniel E. Bürgler, Peter Grünberg

Institut für Festkörperforschung, Forschungszentrum Jülich GmbH, D-52425 Jülich, Germany

Available online 21 October 2004

Abstract

We study a series of NiFe (10.0 nm)/[$Ir_{20}Mn_{80}$ (6.0 nm)/$Co_{80}Fe_{20}$ (3.0 nm)]$_N$ multilayers with different numbers N of bilayers grown by DC magnetron sputtering. After field-cooling, SQUID and MOKE measurements show a sizable increase of the exchange bias field with N. X-ray specular and diffuse scattering data reveal no significant variation of the lateral correlation length and only a weak dependence of the vertical rms interface roughness on N. Atomic and magnetic force microscopy, however, show a strong reduction of the grain size accompanied by distinct changes of the magnetic domain structure. We conclude that the enhancement of the exchange bias effect is related to the shrinking of the domain size in the antiferromagnet due to the structural evolution in the multilayers.

PACS: 68.65.Ac; 75.30.Gw; 75.70.Cn

Keywords: Multilayer; Exchange bias; Microstructure

Magnetic field sensors based on giant magnetoresistance (GMR) in spin-valve structures [1] rely on the exchange bias effect [2], which is employed to fix the magnetization direction of the ferromagnetic reference layer. In spite of its widespread application, exchange bias is not yet fully understood [3,4].

We study exchange bias in [$Ir_{20}Mn_{80}$ (6.0 nm)/$Co_{80}Fe_{20}$ (3.0 nm)]$_N$ multilayers (MLs) with varying number N of ferromagnet/antiferromagnet (FM/AF) bilayers prepared by DC magnetron sputtering. We employ a 10 nm-thick NiFe buffer layer grown on oxidized Si wafers in order to improve the texture of the MLs. All specimens are first annealed at 533 K, i.e. above the Néel temperature $T_N = 520$ K of IrMn, for 60 min in Ar gas and then cooled to room temperature (RT) in an external field of 130 Oe in order to induce the unidirectional anisotropy.

The microstructure and the layer quality are investigated by low-angle X-ray reflectivity (XRR) and X-ray diffuse scattering (XDS) measurements [5] employing a Bruker-axs D8 diffractometer with

*Corresponding author. Fax: +49 2461 61 4443.
E-mail address: a.paul@fz-juelich.de (A. Paul).

0304-8853/$ - see front matter © 2004 Elsevier B.V. All rights reserved.
doi:10.1016/j.jmmm.2004.09.054

Cu-K_α radiation. We measured in specular geometry with the angle of incidence θ_i equal to the exit angle θ_f as well as in off-specular geometry with an offset of $\Delta\omega = 0.13^\circ$ between θ_i and θ_f. True specular reflectivity is obtained by subtracting the off-specularly reflected intensity from the specular one. Diffuse scattering as a function of the in-plane component of the momentum transfer vector is measured by keeping the scattering angle 2θ fixed and rocking the specimen around $\theta_i = \theta_f$. The diffuse scattering measurement provides information about the structure of the interfaces in the film plane. Magnetization loops are recorded by means of a superconducting quantum interference device (SQUID) as well as the magneto-optic Kerr effect (MOKE). Atomic and magnetic force microscopy (AFM/MFM) measurements in tapping mode are performed with a multimode SPM from Digital Instruments using Co-based magnetic tips.

Fig. 1 shows SQUID magnetization loops for different N. There are always two hysteresis loops, one corresponding to the magnetically soft (and interestingly enough always unpinned) NiFe buffer layer and the other to the pinned CoFe layer(s) in the ML. The relative contributions to the sample's total moment confirm this assignment. The averaging over an increasing number of CoFe layers results in slanted loops for larger N. The exchange bias field H_{EB} clearly increases from 330 Oe for $N = 1$ to about 900 Oe for $N = 10$, and it tends to saturate [Fig. 3(c)]. This is even more evident in the MOKE data, where the limited penetration depth of the laser light (about 20 nm) enhances the relative weight of the topmost CoFe layers.

Fig. 2(a) shows true specular reflectivity scans and fits based on procedures described in Refs. [6,7]. The roughness of all IrMn/CoFe interfaces is assumed to be equal and is represented by a single fitting variable σ, and the individual layer thicknesses are fitting parameters. The top CoFe layer is expected to be oxidized, and hence its electron density as well as its thickness are separate fitting

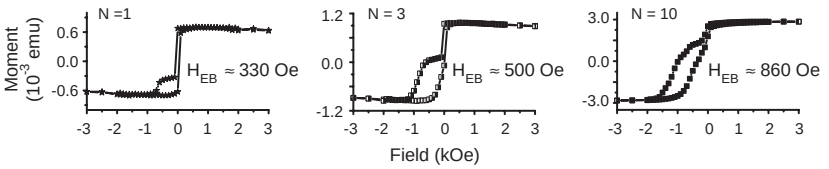

Fig. 1. SQUID magnetization loops of SiO_2/NiFe (10.0 nm)/[IrMn (6.0 nm)/CoFe (3.0 nm)]$_N$ MLs with different numbers of bilayers N. The relative contribution of the FM NiFe buffer decreases and H_{EB} increases with N.

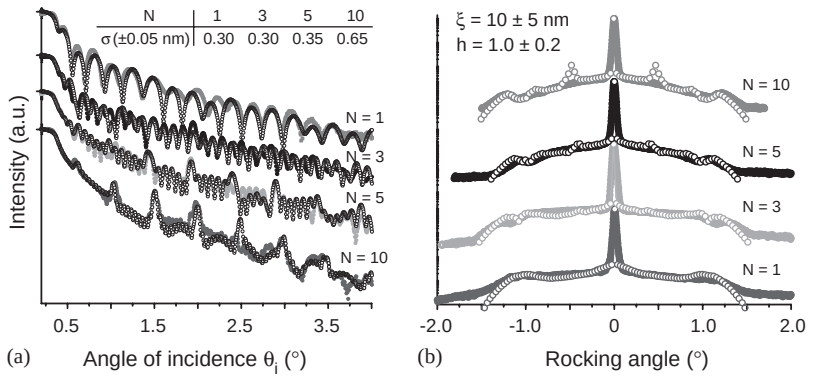

Fig. 2. (a) True specular XRR and (b) XDS at $\theta_i = 1.5^\circ$ of SiO_2/NiFe (10.0 nm)/[IrMn (6.0 nm)/CoFe (3.0 nm)]$_N$ MLs: The fits (open symbols) yield in (a) σ's as indicated and in (b) no significant dependence of ξ and h on N.

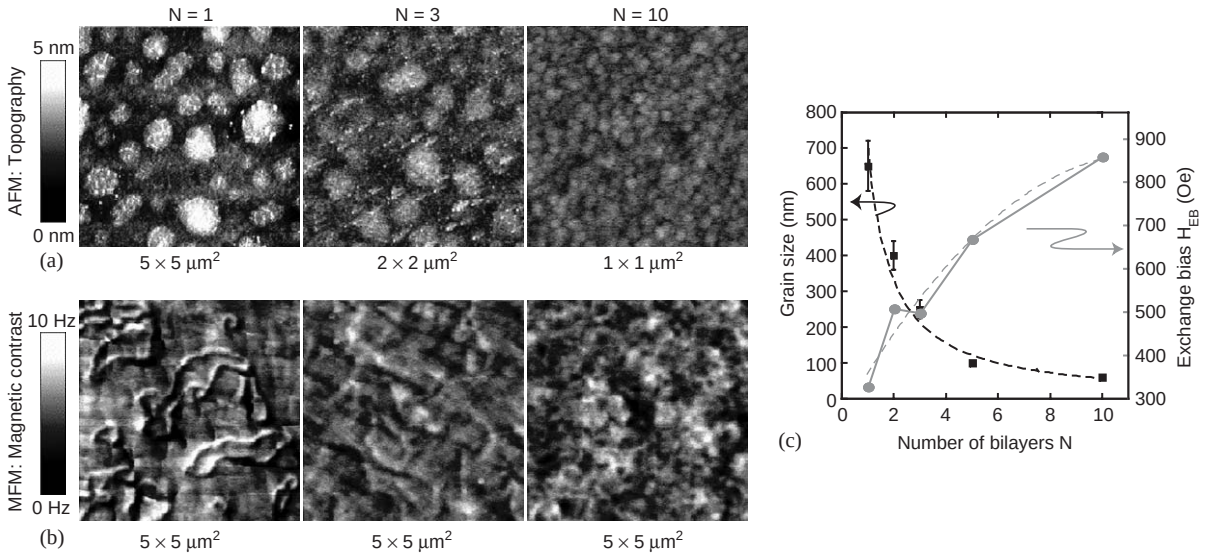

Fig. 3. (a) AFM and (b) MFM micrographs of SiO_2/NiFe (10.0 nm)/[IrMn (6.0 nm)/CoFe (3.0 nm)]$_N$ MLs. MFM images are recorded at zero field after saturating the specimens in the field-cooling direction. Note the different image sizes in (a). (c) Correlation of the dependences of the grain size and H_{EB} on N. Dashed lines are guides to the eyes.

parameters. We do not consider any intermixed layer due to the positive heat of mixing for IrMn and CoFe. The fits yield a rather weak increase of σ from 0.3 to 0.6 nm as N increases from 1 to 10. Variations of σ with N of this order of magnitude are common for multilayers [5,8] and largely depend on the state of the interfaces and the thermodynamics of the elements. The presence of Bragg peaks and total thickness oscillations (Kiessig fringes) in the off-specular reflectivities signifies a high degree of vertical correlation from layer to layer with a vertical correlation length larger than the total ML thickness [9].

Rocking curves and their fits are plotted in Fig. 2(b). Several basic models for the roughness cross-correlation within a ML have been reported in the literature and are discussed in detail in Ref. [5]. We found the best agreement with the model of Holý and Baumbach [9]. It takes into account that interfaces are formed successively from the substrate to the surface and assumes complete correlation. Each interface adds some statistically independent roughness, which is assumed to be completely transferred to all subsequent interfaces. Thus, roughness is accumulated, and σ increases with N. The fitting parameters are σ, the fractal dimension h, and the lateral correlation length ξ. The vertical correlation length κ is found to be larger than the total ML thickness. We observe no significant dependence of h and ξ on N. Moreover, the texture of the MLs as investigated by X-ray diffraction is similar for all N. AFM images shown in Fig. 3(a), however, reveal a strong variation of the grain size from 650 nm for $N = 1$ to 60 nm for $N = 10$ [Fig. 3(c)]. Moreover, the MFM micrographs [Fig. 3(b)] indicate a significant change of the magnetic domain structure with N: The extended domains for $N = 1$ gradually form structures of about 500 nm in diameter for $N = 10$.

We attribute the enhanced H_{EB} to the 10-fold shrinking of the grain size, rather than to the small increase of σ by only 0.3 nm. Due to the absence of long-range dipolar interactions in an AF, domains are stabilized by defects such as grain boundaries. Thus, the smaller grain size at larger N gives rise to smaller AF domains and, thus, a higher density of uncompensated spins, which are aligned during field-cooling and then couple to the FM layer [10,11]. The shrinking of the FM domains with increasing N confirms a link between the grain size and the magnetic ordering. However, we cannot directly correlate AF domains with the observed

FM domains as in Ref. [12], because our samples are field-cooled. Nevertheless, it is likely that the domain state of the AF also changes with grain size, because grain boundaries are energetically preferred sites for AF domain walls.

In conclusion, the structural evolution in $[FM/AF]_N$ MLs leads for increasing N to smaller grains and presumably smaller AF domains, which—as expected in the framework of the domain state model [10]—significantly enhance the exchange bias effect.

References

[1] B. Dieny, J. Magn. Magn. Mater. 136 (1994) 335.
[2] W.H. Meiklejohn, C.P. Bean, Phys. Rev. 105 (1957) 904.
[3] J. Nogués, I.K. Schuller, J. Magn. Magn. Mater. 192 (1999) 203.
[4] A.E. Berkowitz, K. Takano, J. Magn. Magn. Mater. 200 (1999) 552.
[5] A. Paul, G.S. Lodha, Phys. Rev. B 65 (2002) 245416.
[6] L.G. Parratt, Phys. Rev. 95 (1954) 359.
[7] L. Nevot, P. Croce, Rev. Phys. Appl. 15 (1980) 761.
[8] A. Paul, T. Damm, D.E. Bürgler, H. Kohlstedt, S. Stein, P. Grünberg, J. Phys.: Condens. Matter 15 (2003) 2471.
[9] V. Holý, T. Baumbach, Phys. Rev. B 49 (1994) 10668.
[10] U. Nowak, K.D. Usadel, J. Keller, P. Miltényi, B. Beschoten, G. Güntherodt, Phys. Rev. B 66 (2002) 14430.
[11] J. Keller, P. Miltényi, B. Beschoten, G. Güntherodt, U. Nowak, K.D. Usadel, Phys. Rev. B 66 (2002) 14431.
[12] F. Nolting, A. Scholl, J. Stöhr, J.W. Seo, J. Fompeyrine, H. Siegwart, J.-P. Locquet, S. Anders, J. Lüning, E.E. Fullerton, M.F. Toney, M.R. Scheinfein, H.A. Padmore, Nature 405 (2000) 767.